

Multifocusing homeomorphic imaging Part 1. Basic concepts and formulas

Boris Gelchinsky^{a,*}, Alexander Berkovitch^a, Shmariahu Keydar^b

^a *Tel-Aviv University, Department of Geophysics and Planetary Sciences, Ramat Aviv Tel-Aviv 69978, Israel*

^b *The Geophysical Institute of Israel, Baal Shem Tov str 6, Liad, Israel*

Abstract

The decomposition of a total wave field recorded on a set of seismic traces on parts corresponding to different body waves is one of the fundamental problems of data processing. The central point of this problem is the correlation procedure for a seismic event (wave) on a set of recorded traces. In order to implement this procedure, it is necessary to have a local time correction formula for a family of source–receiver pairs arbitrarily distributed around a chosen central pair. This formula is derived in the work for a 2D seismic medium of arbitrary structure using a new homeomorphic imaging method called multifocusing. The presentation of multifocusing is divided into two parts: the basic ideas and concepts of the method, the time correction formula and associated geometrical relationships form Part 1. The main characteristic of the multifocusing approach is the consideration of the geometry of all possible wave fronts, which could be formed in the vicinity of a chosen central source-receiver pair. Provided that a target wave exists on a chosen central trace, then there is also a corresponding central ray and an infinite family of surrounding wave tubes. The basic idea of the multifocusing technique is based on the association of any pair of traces recorded in the vicinity of the central trace with certain ray tube belonging to the family. This association can be always found. Considering this ray tube, the local time correction formula is obtained, assuming a spherical approximation of two tube cross sections at the end points of central ray. In the case of a central ray with non-zero offset, the formula consists of the following parameters: two velocities near the source and receiver locations, two angles (departure and arrival) and two pairs of dual curvatures of tube cross-sections at the ray end points. The first four parameters are common for all traces, the pairs of dual curvatures are, as a rule, specific for the chosen pair of traces; the formula thus obtained could not be directly used in practice. The essential part of the first paper is devoted to the parameterization of the family of dual curvatures. The exact formulas derived for these curvatures include as parameters, a pair of dual curvatures of two chosen fundamental ray tubes. Different choices for the fundamental ray tubes are considered and important relationships between the dual curvatures and spreading functions for these tubes are established. They are the generalization of the Hubral formula [Hubral, P., 1983. Computing true amplitude reflections in a laterally inhomogeneous earth. *Geophysics* 48, 1051–1062] and known reciprocity relations. In the case of a zero-offset central ray, most important for reflection shooting, the formulas derived are significantly simplified and involve four parameters only. The results obtained can be used not only in the multifocusing method, but also in migration and forward modeling. © 1999 Elsevier Science B.V. All rights reserved.

Keywords: Wave field; Multifocusing; Homeomorphic imaging

* Corresponding author. Fax: +972-3-6409282; e-mail: boris@luna.tau.ac.il

¹ Currently at Geoph. Institute, Karlsruhe University.

1. Introduction

A stack of recorded seismic traces became one of the main steps in data processing when multifold acquisition systems were the leading method of collecting seismic data. It seems impossible that a recorded total field could be stacked (or better say, averaged). From physical point of view, meaningful averaging can be achieved with respect to each separate body or surface wave, because it is possible to correct all stacked traces before stacking in such a manner that all target wave events will be “in phase”. Hence, the crucial operation in the stack procedure is time correction. In order to do this properly, it is necessary to have a high quality time correction formula. The term “high quality” is used if the formula satisfies the two following conditions: first, the formula should be valid in the media of arbitrary structure and, second, its accuracy should be sufficiently good when dealing with different acquisition systems. The first condition renders the method applicable to any medium which could be met “in situ”. In practical terms it implies that the time correction formula should be modeled independently. The second condition means, that the formula is valid for an arbitrary distribution of source and receiver pairs.

These two conditions are very general and need to be defined in greater detail. Consider both the properties of propagating body waves and the parameters of existing acquisition systems, the time correction procedure may be divided into the two steps. The first step called “statics” is the correction for an upper zone of rocks with a low velocity and/or rapidly changing seismic properties and a reduction of arrival times to a reference level where the properties can be assumed to be relatively slowly changing. The second stage is the time correction attributed to the reference level. In the following, only this type of time correction is considered. The main theme of this paper concentrates on reflection shooting, although the majority of

relationships obtained are applicable in more general situations.

The creation of the theory of time correction based on a model independent method could be stated as a primary goal from the very beginning when stacking became a necessary procedure. However, the actual development of the time correction theory was carried out in another way. First, the well-known Normal Moveout (NMO) was found for horizontally stratified media. Then, the CMP time correction procedure was improved in the Dip Moveout (DMO) method and associated modifications under the assumption that the velocity model of the overburden is known. The DMO theory was improved by considering models of overburden with increasing complexity. In reality, however, it is very difficult to determine a velocity model of the overburden with sufficient accuracy, especially in most interesting media of complicated structures.

Thus, the conventional approach is based on consideration of specific types of medium models and determination of time correction procedures for them. The latter are used in media of arbitrary structures which, in turn, gives rise to uncertainty as regards their applicability.

A quite different approach is based on the Homeomorphic Imaging (HI) theory (Gelchinsky, 1988, 1989; Keydar et al., 1990, 1996a). It starts from determination of the specific configuration of source-receiver pairs for which an associated wavefront emanating from a target object can be found without assuming the overburden structure. A time correction formula is derived as a result of considering the local geometry of the associated wavefront propagating near a seismic line (source and receiver locations). Each formula obtained is valid in a medium of arbitrary structure. Parameters of the formula are characteristics of the associated wavefront geometry and velocity in the proximity of a seismic line (reference level).

To illustrate the HI technique, consider the Common Reflecting Element (CRE) method

(Fig. 1) (Gelchinsky, 1988). Assume that each source A_k^+ and corresponding receiver A_k^- ($k = 0, 1, \dots, n$) are distributed along a seismic line $A_k^+A_k^-$ in such a way that:

- all rays corresponding to the pairs (traces $A_k^+A_k^-$) have a Common Reflecting Point (CRP);
- a central trace ($A_0^+A_0^-$) \rightarrow (A_0A_0) records a wave normally reflected from a reflector S .

Then, for any 2D medium, the configuration of these rays can be presented in the form of a symbolic ray scheme as shown in Fig. 1a for any 2D seismic medium of arbitrary structure. The term “symbolic” is used in order to emphasize that, in fact, only the existence of such a scheme is needed in the following.

For this ray scheme, a fictitious point source could be placed at the CRP (the point C_0 in Fig. 1b). A fictitious associated wavefront Σ , emitted by this source and reaching the central point A_0 (zero-offset point) at the moment $t_0/2$, is also shown in Fig. 1b. The center of curvature of this associated wavefront, located at the point \hat{C}_0 , is defined as a CRE image of the CRP. The image point \hat{C}_0 and the fictitious wavefront Σ are shown in the image plane in Fig. 1c.

By repeating this procedure for a set of central points, one can obtain the CRE image \hat{S} of the reflector S as a locus of centers of curva-

tures of associated wavefronts emitted by a set of fictitious sources located on the S (Fig. 1c). The boxes and crosses shown in Fig. 1b(1c) correspond to two different positions of the CRP (the image points) on the reflector S (the CRE image \hat{S}). For simplicity’s sake and in order not to complicate the figures, the appropriate central points and ray paths are not shown in Fig. 1b,c.

It could be shown that the reflector S and its CRE image \hat{S} are locally topologically equivalent. This means that each point (or element) of the surface S one-to-one mapped in one point (or element) of the image \hat{S} and vice versa. Following the mathematical terminology, this image is called the CRE homeomorphic image (or simply the CRE homeomorphism) (Gelchinsky, 1988, 1989). The proof of the topological equivalence of the reflector and its group homeomorphic image is given in the paper by Gelchinsky and Keydar, 2000. The proofs for other types of HI images are similarly executed with insignificant changes.

Now we could exploit an obvious property of the proposed mapping: the equality of time increments for the reflected and fictitious wavefronts corresponding to the same locations of source–receiver pairs (Fig. 1a,b). There is indeed only one difference between the above-mentioned figures: the ray directions. On the

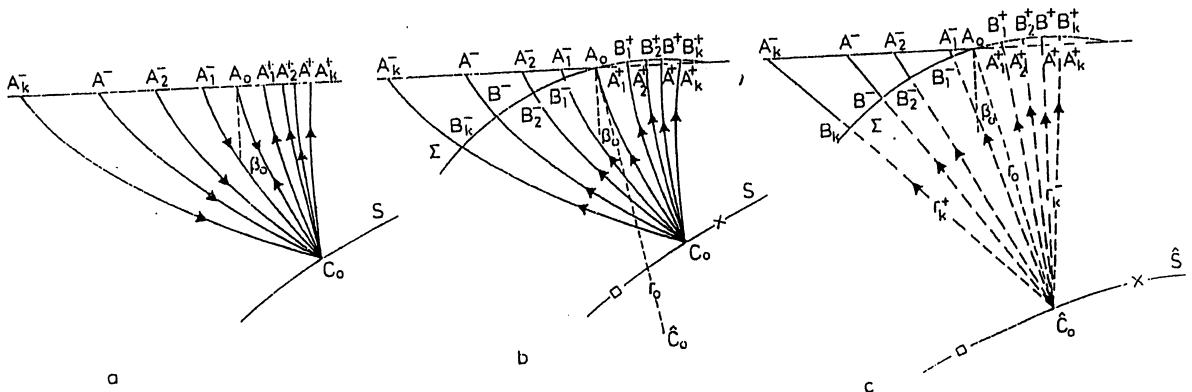


Fig. 1. Ray scheme for the CRE mapping. (a) Ray scheme corresponding to the CRE distribution of source–receiver pairs. (b) Ray scheme corresponding to a fictitious source located at the Common Reflecting Point (CRP). (c) Representation in the image plane the fictitious front and the CRE reflector image \hat{S} .

left parts of Fig. 1a,b they are opposite, so the descending and ascending wave fronts do not coincide (the descending front is not shown on Fig. 1a). However, the time increments $\Delta\tau$ ($A_k^- B_k^-$) and $\Delta\tau$ ($B_k^- A_k^-$) for the descending and ascending wavefronts are equal.

For simplicity's sake, let us sume that the velocity v_0 near the seismic line ($A_k^+ A_0 A_k^-$) is constant and the fictitious wavefront is spherical (Fig. 1c). Strictly speaking, the ray arcs $B_k^\nu A_k^\nu$ ($\nu = +$ or $-$) and the wavefronts Σ on Fig. 1b,c are the same. However for visual estimation of the degree of approximation, these arcs and the front are shown in Fig. 1c taking into account two assumptions. Under these assumptions, it is easy to obtain the following time correction formula (Gelchinsky, 1988; Rabbel et al., 1990; Steentoft and Rabbel, 1992).

$$\begin{aligned}\Delta\tau_k &= \tau(A_k^+ C_0 A_k^-) - \tau(A_0 C_0 A_0) \\ &= \Delta\tau_k^+ + \Delta\tau_k^- \end{aligned} \quad (1)$$

where

$$\begin{aligned}\Delta\tau_k^+ &= \left[\left(r_0^2 + 2r_0 \sin \beta_0 \Delta x_k^+ \right. \right. \\ &\quad \left. \left. + (\Delta x_k^+)^2 \right)^{1/2} - r_0 \right] / 2v_0, \end{aligned} \quad (2)$$

$$\begin{aligned}\Delta\tau_k^- &= \left[\left(r_0^2 + 2r_0 \sin \beta_0 \Delta x_k^- \right. \right. \\ &\quad \left. \left. + (\Delta x_k^-)^2 \right)^{1/2} - r_0 \right] / 2v_0, \end{aligned} \quad (3)$$

and

$$\Delta x_k^\nu = A_k^\nu A_0 = x^\nu - x_0 (\nu = + \text{ or } -). \quad (4)$$

A seismic line is considered as the axis x forming an acute angle of entry β_0 with the central ray $C_0 A_0$ (or $\hat{C}_0 A_0$) of the fictitious wavefront Σ , having a radius r_0 at the point A_0 .

Taking into account Snell's law which governs reflection, it has been shown (Gelchinsky, 1988; Koren and Gelchinsky, 1990) that the offsets Δx_k^+ and Δx_k^- of the k -the source–re-

ceiver pair should be disposed along the seismic line according to the following binomial distributions

$$\Delta x_k^+ = y_k + \alpha (y_k)^2, \quad \Delta x_k^- = -y_k + \alpha (y_k)^2 \quad (5)$$

with y_k is a variable and the coefficient α determined by the formula

$$\alpha = \sin \beta_0 / r_0 + 2 \cos \beta_0 Q'_0 / Q_0^{3/2}, \quad (6)$$

where $Q_0 = Q(\theta = 0)$ and $Q'_0 = Q'(\theta = 0)$ are the 2D spreading function and its derivative with respect to the radiation angle θ at the CRP (C_0), calculated at the central point A_0 . The coefficient α is called a factor of asymmetry (Gelchinsky, 1988).

Where the maximum offset of a gather is rather large, the spherical approximation of the wavefront may be not sufficient. In such a case, a next non-spherical approximation of the associated wavefront should be used (Gelchinsky and Keydar, 1993).

As well known in mathematics, the homeomorphism of a surface is not unique. This means that there are many types of topologically equivalent mapping, and, therefore, other types of reflector mapping using HI images have been proposed. One of these is the Common Evolute Element (CEE) method with a zero-offset source–receiver pair distribution; the others are the Common Source (Receiver) Point (CS-(Rec)P) and Combined HI methods (Gelchinsky, 1989; Keydar et al., 1990, 1993, 1996b). Each type of HI method uses a stack of specifically distributed and time corrected traces. The stacked trace obtained may be regarded as though a field reflected from an interface were focused at an image point corresponding to the type of HI stack performed. This correspondence makes sense only in the context of kinematics and, therefore, it is more correct to call this a quasi-focusing stack. For convenience, however, we will call this stack focusing in the following.

2. The generalization of the HI mapping

All the HI methods mentioned have important merits (such as, enhancing of target waves; preserving resolution; applicability to media of arbitrary structures) but they also have an important drawback. In each method, as in conventional techniques, a stack of about n traces is performed if a n fold acquisition system is used. However a plurality of traces, recorded by this system in the vicinity of a fixed central trace, can be approximated by $(m \times n)$ traces, if each CSP array consists of m traces. Thus, a significant part of the information recorded by the multifold system is not used by these stacking techniques.

In order to increase the amount of traces used, a generalization of the HI technique was proposed (Gelchinsky and Keydar, 1993). According to this generalization, a source and receiver configuration, used in the HI mapping, should possess the following property: a family of rays leaving sources and a related family of rays arriving at receivers should form two-ray congruencies, each of them having an orthogonal front (in the case of isotropic media) in the vicinity of source and receiver locations. This type of mapping may be applied in rather general situations, where sources and receivers are distributed along curved smooth lines arbitrary positioned in a vertical plane with a central ray, non-normally reflected.

One possible configuration, satisfying the formulated conditions, is shown in Fig. 2. This type of HI mapping is associated with two fictitious fronts: one leaving a source line and the other coming to a receiver line. Thus, in the general case the two images are constructed. This type of HI mapping is also used in the Common Converting Element (CCE) method (Gelchinsky, 1989).

The proposed modification of HI mapping significantly enlarges the number of traces that can be used in the stack. However, it does not cover the whole plurality of traces recorded in the vicinity of a fixed central ray. Here we

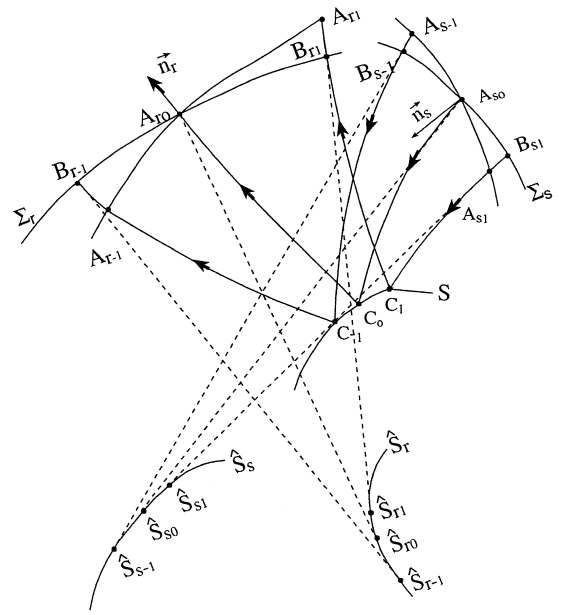


Fig. 2. Ray scheme illustrating homeomorphic imaging for source–receiver pair configuration corresponding to two fictitious fronts. $(A_{s-1}A_{s0}A_{s+1})$ or $(A_{r-1}A_{r0}A_{r+1})$ is the source or receiver line, S is the element of the reflector, C_{-1}, C_0, C_1 are reflection points, $A_{s0}C_0A_{r0}$ is the central ray, Σ_s (Σ_r) is the fictitious front associated with sources (receivers) front, \hat{S}_s (\hat{S}_r) is the element of caustic of the front Σ_s (Σ_r) or the source (receiver) image of the reflector element S .

present a new HI technique, multifocusing, which allows the stack to be utilized by a plurality of traces containing information about a certain area around a particular reflection point.

One can see that the two congruencies of rays, considered earlier, form a ray tube surrounding the fixed central ray (Fig. 2). A cross-section of the ray tube at each end point of the central ray is an element (part) of the one of the mapping wavefronts. The proposed generalization of the HI mapping (Gelchinsky, 1997) comprises an association of any pair of traces with a certain ray tube surrounding the central ray (Fig. 3). The selected pair consists of a fixed central trace $u(A_0^-, A_0^+, t)$ and another trace $u(A_j^-, A_i^+, t)$ selected from a plurality of traces ($i = 0, 1, \dots, m; j = 0, 1, \dots, n$). The two re-

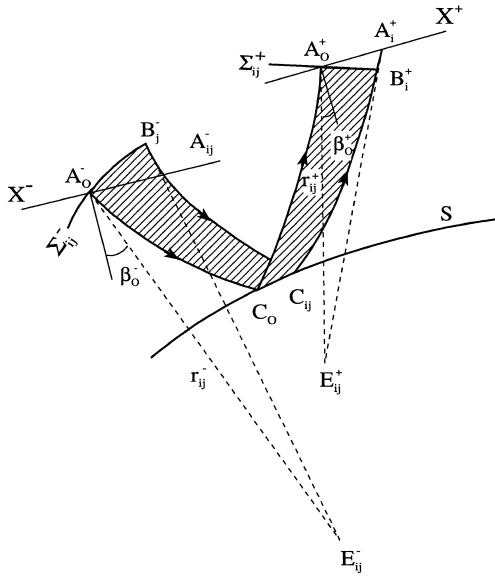


Fig. 3. Ray tube corresponding to a pair of traces (rays). S is the element of reflector, $A_0^- C_0 A_0^+$ is the ray corresponding to the fixed central trace, $A_j^- C_{ij} A_i^+$ is a ray corresponding to a variable trace $u(A_j^-, A_i^+, t)$, $\beta_0^- (\beta_0^+)$ is the angle of departure (arrival) at the central point $A_0^- (A_0^+)$, $\Sigma_{ij}^- (\Sigma_{ij}^+)$ is a front leaving (arriving) the point $A_0^- (A_0^+)$, $r_{ij}^- (r_{ij}^+)$ is the radius of curvature of the front $\Sigma_{ij}^- (\Sigma_{ij}^+)$, $E_{ij}^- (E_{ij}^+)$ is the source (receiver) image point located on a caustic of the front $\Sigma_{ij}^- (\Sigma_{ij}^+)$.

flected rays $A_0^- C_0 A_0^+$ and $A_j^- C_{ij} A_i^+$ correspond to this pair. The dual cross-sections Σ_{ij}^- and Σ_{ij}^+ of the associated ray tube T_{ij} at the points A_0^- and A_0^+ are orthogonal to both selected rays.

It is obvious from a geometrical point of view that this association always exists. If the distances

$$\Delta x_i^+ = x_i^+ - x_0^+ \quad \Delta x_j^- = x_j^- - x_0^- \quad (7)$$

are not very large, a spherical approximation of the wavefront elements Σ_{ij}^- and Σ_{ij}^+ is applicable. In the spherical approximation, the correspondence between the two chosen rays $A_0^- C_0 A_0^+$ and $A_j^- C_{ij} A_i^+$ and the ray tube T_{ij} is unique.

Assuming that radii r_{ij}^- and r_{ij}^+ of the dual spherical fronts Σ_{ij}^- and Σ_{ij}^+ are known, one can derive a formula for the time correction.

The geometrical consideration is similar to that used in the CRE theory by finding the expressions (1)–(3). In this case the time correction is determined by the sum

$$\Delta \tau_{ij} = \Delta \tau_{ij}^- + \Delta \tau_{ij}^+ \quad (8)$$

where the first (second) term is the time correction corresponding to the arc $A_k^- B_k^- (A_k^+ B_k^+)$ of the central ray near the source (receiver). As can be seen from Fig. 3, each term in the last equation is determined by the expressions

$$\Delta \tau_{ij}^+ = A_i^+ B_i^+ / v_0^+, \quad \Delta \tau_{ij}^- = A_j^- B_j^- / v_0^- \quad (9)$$

Thus, in the spherical approximation, we obtain the following formulae:

$$\Delta \tau_{ij}^- = \left[\left((r_{ij}^-)^2 + 2 \sin \beta_0^- r_{ij}^- \Delta x_j^- + (\Delta x_j^-)^2 \right)^{1/2} - r_{ij}^- \right] / v_0^- \quad (10)$$

and

$$\Delta \tau_{ij}^+ = \left[\left((r_{ij}^+)^2 + 2 \sin \beta_0^+ r_{ij}^+ \Delta x_j^+ + (\Delta x_j^+)^2 \right)^{1/2} - r_{ij}^+ \right] / v_0^+ \quad (11)$$

where $v_0^- (v_0^+)$ is the velocity near a source (receiver) location and $\beta_0^- (\beta_0^+)$ is the angle of emission (entry) at the central point $A_0^- (A_0^+)$.

Time correction depends on the parameters $\sin \beta_0^-$, $\sin \beta_0^+$, v_0^- and v_0^+ which are common for all traces recorded around the fixed central points A_0^- and A_0^+ and the two parameters r_{ij}^- and r_{ij}^+ which are specific for the chosen pair of traces $A_0^- A_0^+$ and $A_j^- A_i^+$. For certain collection of traces (like CRE, CEE configurations), the pair of dual radii r_{ij}^- and r_{ij}^+ is the same for all traces belonging to the that configuration. In general, however, values of the radii are different for different pairs. It is useful to note the validity of the formulae (10–11). A simple geometrical consideration used by finding the formulae is applicable to the offsets Δx_i^+ and Δx_j^- , measured along straight (not curved) lines arbitrarily situated in the vertical plane (see, for example, Fig. 2).

The formulae (10)–(11) are not suitable for practical use owing to the a huge number of parameters r_{ij}^- and r_{ij}^+ which is about double the number of traces. It means asymptotically that the number of parameters is infinite.

The main part of this paper is devoted to parameterization of a family of dual radii r_{ij}^- and r_{ij}^+ . It will be shown that this infinite family of radii depends on the abovementioned common parameters and two pairs of basic dual radii.

3. The parameterization of the family of dual wavefront curvature associated with the fixed ray

This section is devoted to the parameterization of the family of the dual curvature at the end points of the fixed ray (Berkovitch et al., 1994; Berkovitch, 1995; Gelchinsky, 1997). The formula derived is valid for any 2D ray having two end points arbitrarily situated in a vertical plane.

Here, we apply the well-known system of linear equations of dynamic ray tracing (Červený, 1985). The consideration in this section is performed at the mathematical level. The procedure for formulae derivation and the notation used seem, at first glance, a little sophisticated, although the proposed idea and technique used are simple. We decided, therefore, to present the idea and a short scheme of derivation at the beginning of this section.

It has been shown that the ray tube T surrounding a fixed central ray can be associated with two source–receiver pairs corresponding to two traces. The dual radii of the cross-sections of the ray tube at its end point are the parameters in the time correction formulae (10)–(11). Those formulae determine a time correction of one current pair of traces with respect to a central trace. Each of the sets of ray tubes and the corresponding dual radii pairs is asymptotically infinite. Our aim is to determine formulae

expressing the pair of dual radii using two pairs of dual radii designated as basic. It is convenient from a technical point of view to consider the wavefront curvature k instead of the radius r in the following.

The ordinary equation governing the change of curvature along a fixed ray could be used to find the abovementioned formulae. However this equation is a nonlinear, Riccati types (Červený, 1985, p. 42 Eq. (5).15) and Riccati equations are very difficult to handle. We have, therefore used another way.

The well-known system of dynamic ray tracing is used for finding the abovementioned formulas. In the dynamic ray tracing approach, the curvature is expressed by the ratio (Eq. (12) in the following) of two functions, the one is Q , which is the geometrical spreading, and the another, P , that is connected with a change of angles between rays. The functions Q and P satisfy the system of two linear Eq. (13). A general solution $Q(t)$ and $P(t)$ of the system is presented as a superposition (14) of the two basic solutions Q_1, P_1 and Q_2, P_2 with arbitrary constant a and b . It means that an arbitrary pair of curvature (or the functions $Q(t)$ and $P(t)$) can be found using a) the formulas (14) and (12) with a help of the two basic solutions $Q_i(t)$ and $P_i(t)$ ($i = 1$ or 2) or b) the superposition formula (15) obtained from the relations (14) and (12) with a help of the two basic wavefront curvatures $k_1(t)$ and $k_2(t)$.

In order to find the expressions for the constants a and b , the basic solutions Q_1 and Q_2 are chosen, using a special type of the boundary conditions (18) at the ray end points. One of them is called the ES (equal spreading) solution, because the cross-sections of the corresponding ray tube T_c at the ray end points are equal. The another solution is called AES (anti-equal spreading) solution, since the spreading at the end points of the ray tube T_a have the equal modules and the opposite signs. It is shown in the process of the derivation, that the superposition formula (15) can be transformed to the Eq. (20) giving the parametric description of the

family of the dual curvatures with a help of the two basic dual curvatures at the end points of the fixed ray.

The derived formulas (20) for the curvatures of the end cross-sections of an arbitrary ray tube allow to go to the further consideration of multi-focusing theory. The proposed approach can be also applied to finding many useful expressions in the case of different source–receiver configurations. In particular, it is shown (the relations (23)), that a curvature of a front radiated by a point source located at one end point of the central ray and recorded at the another end point is equal to a half-sum of the curvature of the ES and AES wavefronts at the recording points.

Then the other pair of solutions of the linear system (13) is chosen as a basic one. In this case, the basic solutions Q_{p_μ} and P_{p_μ} correspond to the point source located at the point A_μ . As result of algebraic manipulations with the superposition formula (15), the formulas (28)–(29) determining the relation between the inverse spreading $q = 1/Q$ in the case of a point source and the curvatures of the ES and AES wavefronts are found. These formulas are a generalization of the Hubral formula (Hubral, 1983) for cases when a central ray has not-coincident end points.

Now we set to the detailed consideration of the circumscribed above scheme. As it was said before, the well-known system of equations of dynamic ray tracing is used (Červeny, 1985 p. 43 Eq. (5).23). The system governs the behavior of two functions $Q(t)$ and $P(t)$ associated with a wavefront curvature by the relation

$$k(t) = v(t)P(t)/Q(t), \quad (12)$$

where t is the time of propagation along the ray measured from an original point M_0 to a current point $M(t)$ and $v(t)$ is the velocity at the point $M(t)$.

The function $Q(t)$ is called spreading function because it is equal to a square of a geometrical spreading of a surrounding ray tube. The function $P(t)$ is connected with a change of angles between rays.

The dynamic ray tracing system has the form

$$\frac{dQ}{dt} = vv_s P, \quad \frac{dP}{dt} = -vv_l Q, \quad (13)$$

where v_s is the first derivative of v in the direction s along the ray and v_l the second derivative of v in the direction l orthogonal to the ray.

A general solution of the system (13) can be presented as a superposition

$$Q(t) = aQ_1(t) + bQ_2(t), \quad P(t) = aP_1(t) + bP_2(t) \quad (14)$$

of the two basic solutions: Q_1 , P_1 and Q_2 , P_2 with arbitrary constants a and b . A choice of some particular solution is carried out by assigning special values to a and b .

After substitution Q and P from the Eq. (14), the expression (12) takes the form

$$k(t) = v(t)[aP_1(t) + bP_2(t)] / (aQ_1(t) + bQ_2(t)), \quad (15)$$

which is transformed by simple manipulations to the relation

$$k(t) = [k_1(t) + \sigma_\gamma k_2(t)] / [1 + \sigma_\gamma(t)], \quad (16)$$

where

$$\sigma_\gamma(t) = \gamma Q_2(t)/Q_1(t), \quad \gamma = b/a. \quad (17)$$

$k_1(t)$ and $k_2(t)$ are basic curvatures corresponding to two basic solution in formula (14) Now we specify a choice of the basic solution. The basic spreadings $Q_1 = Q_e$ and $Q_2 = Q_a$ are chosen according to the following condition determined at the ray end points $A^-(t=0)$ and $A^+(t=t_0)$

$$Q_e^+ = Q_e^- = Q_0, \quad Q_a^+ = -Q_a^- = Q_0, \quad (18)$$

where

$$Q_\kappa^+ = Q_\kappa(A^+), \quad Q_\kappa^- = Q_\kappa(A^-) \quad (\kappa = e \text{ or } a). \quad (19)$$

The function Q_e is called the equal spreading (ES) solution because the spreadings (cross-sections) of the corresponding ray tube T_e are equal

at the ray end points. The function Q_a is named the anti-equal spreading (AES) solution because the spreadings at the end points have the equal modules and the opposite signs. In the following entities referring to the ES and AES solution are labeled by the subscripts e and a correspondingly.

Using the conditions (18) we transform the relation (16) to the form

$$k_\gamma^+ = \frac{k_e^+ + \gamma k_a^+}{1 + \gamma}, \quad k_\gamma^- = \frac{k_e^- - \gamma k_a^-}{1 - \gamma} \quad (20)$$

The expression (20) give a parameterized description of the family of the dual curvatures at the end points of the fixed rays. The parameters are the two pairs of curvatures: k_e^+, k_a^+ and k_e^-, k_a^- . The derived expressions serve as a satisfactory basis for the further consideration of the multifocusing. However, the expressions (15)–(17) could also be applied for finding many important and useful relations between spreading functions and wavefront curvatures for different source–receiver configurations.

Let us consider a point source located at one of the end points A^ν , ($\nu = +$ or $-$) and labeled by a subscript p_ν . The boundary conditions can be written in the form

$$Q_{p_\nu}^\nu = 0, \quad Q_{p_\nu}^\nu k_{p_\nu}^\nu = 1, \quad P_{p_\nu}^\nu = 1/\nu_\nu \quad (21)$$

Taking into account that a curvature $k_{p_\nu}^\nu$ is infinite at the point A^ν , we obtain from the Eqs. (17), (20) and (21) the following relationships for the coefficients a , b and γ

$$\gamma_{p_+} = -1, \quad \gamma_{p_-} = 1, \quad a_{p_+} = -b_{p_+}, \quad a_{p_-} = b_{p_-} \quad (22)$$

and the important formulas

$$k_{p_+}^- = (k_e^- + k_a^-)/2, \quad k_{p_+}^+ = (k_e^+ + k_a^+)/2 \quad (23)$$

for the dual curvatures.

Eq. (23) shows that a curvature of a wavefront, emitted by a point source located at one

end point of the ray and recorded at another end point, is equal to a half-sum of the curvatures of the ES and AES fronts at the point of recording.

It is convenient for the following to change the basic solutions Q_1, r_1 and Q_2, r_2 , selecting the point source wavefronts as the basic ones:

$$Q_1 = Q_{p_+}^+ = 0, \quad k_1 = k_{p_+}^+ = \infty, \quad Q_2 = Q_{p_-}^- = 0, \quad k_2 = k_{p_-}^- = \infty. \quad (24)$$

The selected basis corresponds to the boundary conditions (21). Using these conditions and the Eq. (14), we find the relations

$$Q^+ = bQ_{p_-}^+, \quad Q^- = aQ_{p_+}^- \quad (25)$$

for the general solution (14) and

$$b_e Q_{p_-}^+ = a_e Q_{p_+}^-, \quad b_a Q_{p_+}^+ = -a_a Q_{p_-}^- \quad (26)$$

for the ES and AES solutions determined by the Eq. (18). Using the expressions (17) and (26) we find the following formulas

$$\gamma = \gamma_e = b_e/a_e = Q_{p_+}^-/Q_{p_-}^+, \quad \gamma_a = -Q_{p_+}^-/Q_{p_-}^+ = -\gamma \quad (27)$$

Substituting the values γ_e and γ_a from Eq. (27) into Eq. (15), obtaining equations for a curvature k_e^ν and k_a^ν and solving for $Q_{p_+}^-$ and $Q_{p_-}^+$, we find

$$q_{p_+}^- = 1/Q_{p_+}^- = (k_e^+ - k_a^+)/2, \quad (28)$$

and

$$q_{p_-}^+ = 1/Q_{p_-}^+ = (k_e^- - k_a^-)/2 \quad (29)$$

The derived formulas show that an the inverse spreading q of a wavefront, emitted by a point source located at one ray end point and observed at another end point, is equal to a half differences between curvatures of the ES and AES wavefronts, propagating in the opposite direction from the observation point to the source location.

In order to complete considerations of the formulas binding curvatures and spreading functions in different cases, we recall the reciprocity

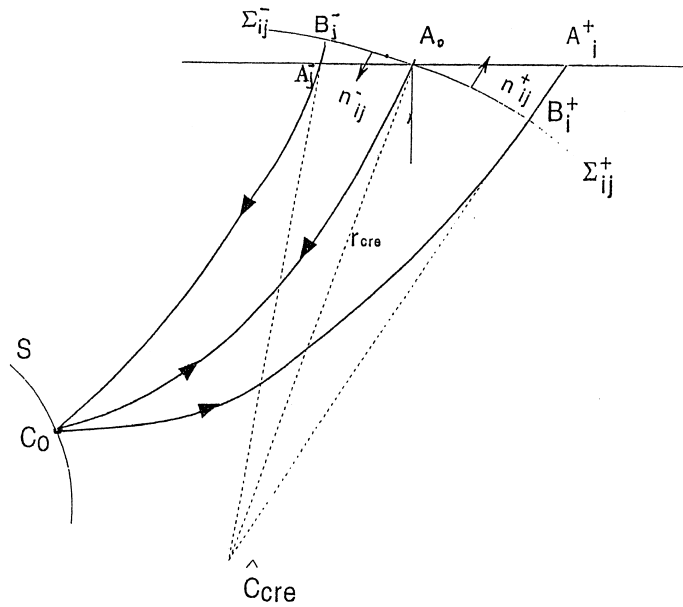


Fig. 4. Ray tube corresponding to the CRE configuration. S is the element of reflector; $A_0C_0A_0$ is the normally reflected ray related to the central trace $u(A_0, A_0, t)$; $A_j^-C_0A_i^+$ is a reflected ray corresponding to the trace $u(A_j^-, A_i^+, t)$; Σ_{ij}^- (Σ_{ij}^+) is the element of the fictitious front leaving (arriving) the point A_0 in the direction of the normal \mathbf{n}_{ij}^- (\mathbf{n}_{ij}^+); r_{cre} is the radius of curvature of the front Σ_{ij}^+ ; \hat{C}_{cre} is the CRE image of the CRP(point C_0).

relation for the spreading function (Červeny, 1987, p. 6.25, Eq. (2); see also pp. 6.24–6.25)

$$Q_{p-}^+ / v^+ = Q_{p+}^- / v^- \tag{30}$$

Substituting the spreading function from the last formulas in Eqs. (28) and (29), we obtain the relation

$$(k_e^+ - k_a^+) / v^+ = (k_e^- - k_a^-) / v^- \tag{31}$$

Taking into consideration the last relation, we see that only three quantities of the four curvatures k_e^ν and k_a^ν ($\nu = +$ or $-$) entered as parameters in expression (20), are independent.

Similarly, relation (31) could be considered as a reciprocity principle for the differences in curvature of the ES and AES wavefronts.

If a plane wavefront element labeled by the subscript π_+ or π_- leaves point A^+ or A^- , then one of the conditions $k_{\pi_+}^+ = 0$ or $k_{\pi_-}^- = 0$ is satisfied. Using these conditions and the expression (20), we obtain the relations

$$\gamma_{\pi_+} = -k_e^+ / k_a^+, \quad \gamma_{\pi_-} = k_e^- / k_a^- \tag{32}$$

Substituting the values from the last formulas in Eq. (20), we find the equations

$$k_{\pi_+}^- = \frac{k_e^- k_a^+ + k_e^+ k_a^-}{k_e^+ + k_a^+}, \tag{33}$$

$$k_{\pi_-}^+ = \frac{k_e^- k_a^+ + k_e^+ k_a^-}{k_e^- + k_a^-} \tag{34}$$

The interesting relation

$$k_{\pi_-}^+ k_{\pi_+}^- = k_{\pi_+}^+ k_{\pi_-}^- \tag{35}$$

follows from Eqs. (23), (33) and (34). It could be interpreted as a reciprocity relation for a product of curvatures of wavefronts, observed at the two ray end points and originating from a point source and plane wave at the opposite end points.

4. Parameterization of a family of wavefront curvatures for normally reflected ray

The expressions derived for a family of dual curvatures and their spreads are essentially sim-

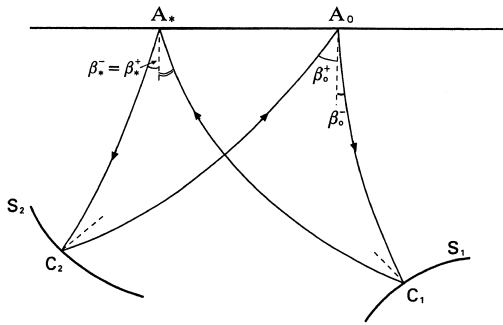


Fig. 5. Ray scheme for multiple corresponding to the zero-offset configuration of source–receiver pairs. S_1 (S_2) is the first (second) reflector; $A_0C_1A^*C_2A_0$ is the double circle ray of multiple, in general, the angle departure β_0^- is not equal to the angle of entry, i.e., $\beta_0^- \neq \beta_0^+$.

plified in the most interesting special case, while the end points A_0^+ and A_0^- coincide and the fixed ray is a normally reflected ray.

Using a geometrical consideration, it is possible to show that in this special case the ES (and AES) ray tube goes to the CEE (and CRE) ray tube.

In order to illustrate this point, it is necessary to reinterpret the CRE ray scheme, shown in Fig. 1, in the terms of a ray tube T_{cre} , having the two cross-sections at the endpoint $A_0^- \rightarrow A_0$ (the left side of the tube in the Figs. 1 and 4) and at the end point $A_0^+ \rightarrow A_0$ (the right side of the tube in Figs. 1 and 4). Dividing the fictitious wavefront Σ at the central point A_0 (Fig. 1) into left and right parts, we can consider its left part as one end cross-section Σ^+ of the ray tube T_{cre} , corresponding to a wave traveling to the CRP, and its right part as another end cross-section Σ^- related to a wave arriving at the CRP (Fig. 4).

In this case, the spreadings Q_{cre}^+ and Q_{cre}^- corresponding to the sections Σ^+ and Σ^- are bound by the relation

$$Q_{cre}^+ = -Q_{cre}^- \text{ at the point } A_0 \quad (36)$$

because the CRP is a focusing point. This relation coincides with condition (18) for the AES tube in the general case. It is also clear from

Figs. 1 and 4, that the angles of emission and entry and the curvatures of the end cross-sections are linked by conditions

$$\beta_0^+ = \beta_0^- = \beta_0, \quad k_{cre} = k_a^+ = -k_a^- \quad (37)$$

Addressing the CEE ray scheme (Gelchinsky, 1989; Keydar et al., 1990; Gelchinsky and Keydar, 2000) and applying a geometrical consideration similar to that used above, we find the boundary conditions

$$\beta_0^+ = \beta_0^- = \beta_0, \quad Q_{cee}^+ = Q_{cee}^-, \quad k_{cee} = k_e^+ = -k_e^- \quad (38)$$

for the CEE case.

It is important to note, that the conditions (37) and (38) correspond to a normally reflected ray and they are not satisfied for most types of multiples (Fig. 5).

In the general case, the inequalities

$$\beta_0^+ \neq \beta_0^-, \quad |k_e^+| \neq |k_e^-|, \quad |k_a^+| \neq |k_a^-| \quad (39)$$

are true for multiples, even if the ray end points coincide. Only in horizontally stratified media are there symmetrical multiples, which is invariant with respect to a change in succession of points of reflection, the conditions (37) and (38) are valid, if the end points coincide (Fig. 6).

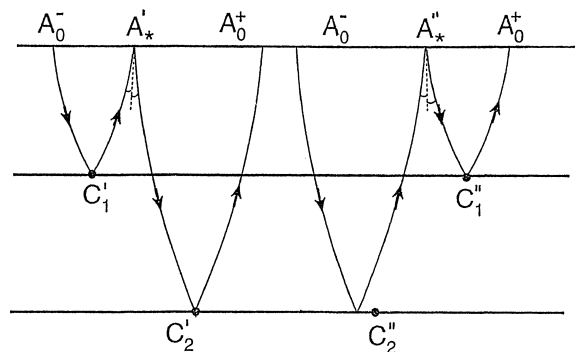


Fig. 6. Ray schemes for the two versions (analog) of the same type of multiple in a horizontally stratified medium. The corresponding angles of departures and entry are equal in the both cases, because seismic properties of the model at the points A^* , C_1' , C_2'' and the points A'' , C_1'' , C_2'' correspondingly are equal.

Due to conditions (37) and (38) the expressions for wavefront curvatures and spreading functions are simplified. Expressions (20) take the forms

$$k_{\gamma}^{+} = \frac{k_{\text{cee}} + \gamma k_{\text{cre}}}{1 + \gamma}, \quad k_{\gamma}^{-} = \frac{k_{\text{cee}} - \gamma k_{\text{cre}}}{1 - \gamma}, \quad (40)$$

It is useful to bear in mind that the signs of the wavefront curvature k^{-} in Eqs. (20) and (40) correspond to the sign of the incident wave front (Fig. 4) formed by sources and is opposite to the sign of curvature of a fictitious wavefront which is entered into the formulae for time correction (9) and (11).

The formulae for the wavefront curvature (23) and the inverse spreading (28)–(29) in the case of the point source are transformed to the relations

$$k_p = (k_{\text{cee}} + k_{\text{cre}})/2, \\ q_p = 1/Q = (k_{\text{cee}} - k_{\text{cre}})/2 \quad (41)$$

The equation for q_p was first obtained by Hubral (1983). He proposed to use it for a so-called true amplitude construction. Using the second formula from Eq. (41), one could correct the observed amplitudes of reflected waves for the geometrical spreading if the curvatures k_{cee} and k_{cre} are determined with the help of some technique (for instance, by an optimal stack) (Tygel et al., 1992). This true amplitude technique is successfully used in reflection wave processing (Schleicher et al., 1993). The expressions (33)–(34) for the radius of the wavefront curvature recorded at one end of the ray tube T_{pi} , if a plane wave element is entering on other side, can be transformed to the formula

$$r_{\pi_{-}}^{+} = 1/k_{\pi_{-}}^{+} = (r_{\text{cee}} + r_{\text{cre}})/2 = r_{\pi_{+}}^{-}. \quad (42)$$

for the radius of the wavefront curvature. An interesting result is obtained if the radius of one cross-section of a ray tube is infinite, then the radius of another tube cross-section is equal to half the sum of the radii of the CEE and CRE wavefronts.

5. Discussion and conclusions

This work was originally started with a view to finding a local time correction formula for a set of seismic traces arbitrarily distributed around each central trace recorded by a multi-fold acquisition system in a 2D medium. We took, as a basis, the geometrical HI approach, which considers the geometry of wave fronts associated with a special configuration (CRE, CEE, CSP etc.) of source–receiver pairs. The generalization proposed in the paper is an association of each pair of traces (one is a fixed central trace and the second is any trace, taken in the vicinity of the first) with a certain ray tube surrounding a central ray connecting the central source and receiver. It is very easy, in such a general approach, to find (in a spherical approximation of cross-sections of the ray tube at the central ray end points) the time correction formula for source–receiver pairs arbitrarily distributed along two straight lines located in the vertical plane. In order to render the formula suitable for practical use, we find the parameterization of an infinite family of all possible pairs of dual curvatures of the ray tube cross-sections. The resulting solution depends on the pair of the dual curvatures of two fundamental ray tubes.

The general approach proposed facilitates deriving not only the time correction formula needed for multifocusing, but also finding a set of very important relationships between curvatures and spreading functions of ray tubes for different configurations of sources and receivers located on two straight lines. These relations enable us to find the spreading function for the CSP configuration for each central ray connecting two points on these lines, as one of parameters of multifocusing processing of recorded data (one choice of basic ray tubes). Using another choice of basic dual curvatures, the spreading function is calculated with the help of the derived relationships (Eqs. (28) and (29)), which are the generalization of the Hubral formula (Hubral, 1983) on an arbitrary configuration of source–receiver pairs in the vertical

plane. Multiplying each wave field by the calculated spreading function, a so-called true amplitude of wave field can be determined. This true amplitude can be attributed to some wave field formation propagating without geometrical spreading. This formation can be called a pseudo-plane wave, taking into account that a major characteristic of plane waves is propagation without geometrical spreading. The pseudo-plane wave also propagates in an elastic medium between interfaces with an invariable amplitude, which is equal to the product of refraction and reflection coefficients along the central ray.

The possibility of finding corrected traces formed by pseudo-plane waves by processing recorded wave fields, opens up a very good prospect for a migration method. The results obtained also permit modifying the formulation of a forward problem and computational algorithms in cases of multifold acquisition systems situated on two lines (see, for example, Koren and Gelchinsky, 1990). While modeling wave fields of a body wave in the case of multifold system, one could restrict oneself to the calculation of kinematic attributes and amplitudes of a pseudo-plane wave along of a set of selected central rays. The kinematic attributes include: propagation time between end points of the chosen central rays, angles of departure and entry and a pair of dual curvatures corresponding to two chosen basic ray tubes. For example, in the case of reflection shooting, the CRE and CEE curvatures (or Q and P functions) at the end points of normally reflected rays can be chosen as a pair of basic parameters. Knowing the kinematic attributes of a pseudo-plane wave, it is possible to determine the travel time for a ray connecting any pair of points situated on the end lines using the formulae derived in the paper. In a spherical approximation applied, there is only one restriction on the length of source and receiver offsets.

The results obtained have paved the way to significant improvements in solving kinematics inverse problem (Berkovitch and Gelchinsky,

1989; Gelchinsky and Keydar, 1993). The dual and reciprocity relationships could be used as certain control conditions through the construction of the “true” kinematics seismic model.

References

- Berkovitch, A., Gelchinsky, B., 1989. Inverse of Common Reflecting Element data: 59th Ann. Intern. Mtg., Soc. Exp. Geophys., Expanded Abstracts, 1250–1253.
- Berkovitch, A., Gelchinsky, B., Keydar, S., 1994. Basic formulae for multifocusing stack: 56th Mtg. Eur. Assoc. Expl Geophys., Extended Abstracts, Session, p. 140.
- Berkovitch, A., 1995. The multifocusing method for homeomorphic imaging and stacking of seismic data, PhD thesis, Tel-Aviv Univ.
- Červený, V., 1985. The application of ray tracing to the numerical modeling of seismic wave fields in complex structures. In: Dohr, G. (Ed.), *Seismic Shear Waves, Part A: Handbook of Geophysical Exploration*, 15. Geophysical Press, 1–124.
- Červený, V., 1987. *Ray Method for Three-Dimensional Seismic Modeling*, Petroleum Industrial Course, The Norwegian Institute of Technology, Trondheim.
- Gelchinsky, B., 1988. Common Reflecting Element (CRE) method. *Explor. Geophys.* 19, 71–75.
- Gelchinsky, B., 1989. Homeomorphic imaging in processing of seismic data (fundamentals and schemes): 59th. Ann. Intern. Mtg., Soc. Exp. Geophys., Expanded Abstracts, 983–988.
- Gelchinsky, B., 1997. Special Course on Homeomorphic Imaging given in connection with “Karlsruhe Workshop on Amplitude-Preserving Seismic-Reflection Imaging” organized by Geophysical Institute, Karlsruhe Univ.
- Gelchinsky, B., Keydar, S., 2000. Homeomorphic Imaging: Theory and Practice: the present issue.
- Gelchinsky, B., Keydar, S., 1993. Basic HI formulas of general theory of local time correction: 63rd Ann. Intern., Soc. Exp. Geophys., Expanded Abstracts, 1145–1448.
- Hubral, P., 1983. Computing true amplitude reflections in a laterally inhomogeneous earth. *Geophysics* 48, 1051–1062.
- Keydar, S., Gelchinsky, B., Shtivelman, V., Berkovitch, A., 1990. The Common Evolute Element (CEE) stack method (zero-offset stack): 60th Ann. Intern. Mtg., Soc. Exp. Geophys., Expanded Abstracts, 1911–1913.
- Keydar, S., Gelchinsky, B., Berkovitch, A., 1993. The Combine Homeomorphic Stacking method: 63rd Ann. Intern., Soc. Exp. Geophys., Expanded Abstracts, 1141–1144.

- Keydar, S., Edry, Berkovitch, A., Gelchinsky, B., 1996a. Construction of kinematic seismic model by homeomorphic imaging method: 57th EAEG Conf. and Tech. Exh., Extended Abstracts, 80–86.
- Keydar, S., Gelchinsky, B., Berkovitch, A., 1996b. Common shot point stacking and imaging method. *J. Seismic Explor.* 5, 261–274.
- Koren, Z., Gelchinsky, B., 1990. Common Reflecting Element (CRE) ray tracing for calculation of global multi-offset time field. *Geophys. J. Int.* 99, 391–400.
- Rabbel, W., Bittner, R., Gelchinsky, B., 1990. Seismic mapping of complex reflectors with Common Reflecting Element (CRE) method. *Phys. Earth Planet. Inter.* 67, 200–210.
- Schleicher, J., Tygel, M., Hubral, P., 1993. 3D true-amplitude finite-offset migration. *Geophysics* 58, 1112–1126.
- Steentoft, H., Rabbel, W., 1992. The CRE method: a technique of homeomorphic imaging in processing of seismic data. *Acoust. Imaging* 19, 803–809.
- Tygel, M., Schleicher, J., Hubral, P., 1992. Geometrical-spreading correction of offset reflections in a laterally inhomogeneous earth. *Geophysics* 57, 1054–1063.